Reeb chart unfolding based 3D shape signatures

Julien Tierny, Jean-Philippe Vandeborre, Mohamed Daoudi

Reeb chart unfolding based 3D shape signatures

Julien Tierny[1], Jean-Philippe Vandeborre[1,2] and Mohamed Daoudi[1,2]
[1] LIFL (UMR USTL/CNRS 8022), University of Lille, France
[2] GET / TELECOM Lille 1
{tierny, vandeborre, daoudi}@lifl.fr

Abstract

This paper presents a novel surface parameterization based technique that addresses the pose insensitive *shape signature problem for surface models of arbitrary genus. It is based on the key idea that two surface models are similar if the canonical mappings of their sub-parts introduce similar distortions.*
First, a Reeb graph of the shape is computed so as to segment it into charts of controlled topology, denoted as Reeb charts*, that have either disk or annulus topology. Next, we define for each Reeb chart a straightforward mapping to the canonical planar domain. Then, we compute a* stretching signature *of the canonical mapping based on an area distortion evaluation. Finally, the input shape is represented by the set of the stretching signatures. An application to pose-insensitive shape similarity is proposed by comparing the signatures of the different Reeb charts.*
Promising experimental results are presented and compared to state-of-the-art techniques. The gain provided by this new signature as well as its interest for partial shape similarity are demonstrated.

Keywords: *Shape analysis, shape signature, Reeb graph, surface parameterization.*

1. Introduction

Shape signatures are compact representations that encode most of the shape characteristics. They are the key ingredient of content-based shape retrieval systems. Such systems take advantage of the signature conciseness to speed up the shape similarity estimation process, benefiting many applications like interactive modeling by example [FKS*04]. A fundamental feature of a shape signature is its stability against transformations of the represented shape, enabling shape retrieval systems to match similar shapes modulo these transformations.

A challenging open issue is the definition of efficient 3D shape signatures that are robust to rigid and *non-rigid* transformations, such as character articulation or shape bending. Structural based signatures [HSKK01] are interesting candidates, particularly because they represent the shape as a set of distinctive sub-parts and thus can address an additional challenging issue, which is partial shape retrieval [BMSF06]. However, in that kind of approach, an appropriate signature still has to be defined for each of the identified sub-parts. Among the other existing *pose insensitive* 3D shape signatures (based on geodesic distance distributions [GSCO07], topological point rings [TL07] or spectral analysis), surface parameterization based techniques sound particularly promising as they already gave excellent results for face recognition [WWJ*06]. They aim at describing the intrinsic 2D information carried by the underlying surface model independently from its 3D spatial embedding (or its pose). However, a major drawback of these techniques is that the topology of the surfaces to compare must be fully controlled (the surfaces must be topology equivalent).

In this paper, we propose a novel surface parameterization based technique that addresses the pose insensitive shape signature problem. This work makes the following contributions. It improves previous parameterization based techniques by being able to handle surfaces of arbitrary genus. It also improves previous decomposition based techniques by proposing more efficient sub-part signatures. It is based on the key idea that two surface models are similar if their sub-parts, or *Reeb charts*, are similar (in particular, if their mappings to the canonical planar domain introduce similar distortions).

After a brief method overview, we define the so-called Reeb charts and introduce the Reeb chart unfolding signatures. Finally, we propose an application to pose-insensitive shape similarity estimation. We present experimental results that demonstrate the gain of the proposed signature for global shape retrieval and we give early results showing its interest for partial shape retrieval.

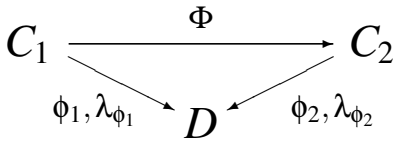

Figure 1: *Reeb chart similarity estimation process: each chart C_i is mapped under ϕ_i to the canonical planar domain D and its stretching signature λ_{ϕ_i} is computed with regard to the area distortion introduced by ϕ_i.*

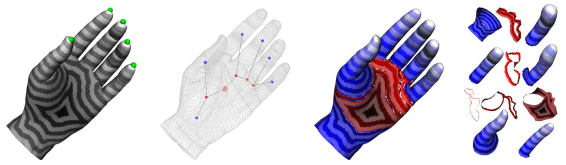

(a) (b) (c) (d)

Figure 2: *Segmentation of a hand surface model into its Reeb charts.*

2. Method overview

Let M be a closed 2-manifold of arbitrary genus embedded in $\mathbb{R}^3$. First, we compute the Reeb graph of M to segment it into a set of charts C_i of controlled topology, that we call *Reeb charts*, that have either disk or annulus topology.

To evaluate the similarity between two charts C_1 and C_2 of equivalent topology, we try to characterize a map $\Phi : C_1 \rightarrow C_2$. However, in this paper, we focus on signature computation. Hence, we characterize Φ using the transition mappings ϕ_1 and ϕ_2 to the canonical planar domain D (either the unit disk or the unit annulus) as shown in figure 1: $\Phi := \phi_2^{-1} \circ \phi_1$. Then, the similarity between C_1 and C_2 is evaluated by comparing the mappings ϕ_1 and ϕ_2. In particular, we characterize ϕ_1 and ϕ_2 by their *stretching signature* (λ_{ϕ_1} and λ_{ϕ_2}), a function of the area distortion they introduce.

Then, for shape similarity estimation purposes, we introduce a distance between the stretching signatures λ_{ϕ_1} and λ_{ϕ_2}. Finally, the distance between two closed 2-manifolds of arbitrary genus is a function of the stretching signature distances associated to their different Reeb charts.

3. Reeb chart segmentation

To deal with surfaces of arbitrary genus, we use a divide-and-conquer strategy based on Reeb graphs (see definition 1), as proposed within the framework of triangulation remeshing [PSF04] or texture mapping [ZMT05].

Definition 1 (Reeb graph) Let $f : M \rightarrow \mathbb{R}$ be a Morse function defined on a compact manifold M. The Reeb graph $R(f)$ is the quotient space on $M \times \mathbb{R}$ by the equivalence relation $(p_1, f(p_1)) \sim (p_2, f(p_2))$, which holds if $f(p_1) = f(p_2)$ and p_1, p_2 belong to the same connected component of $f^{-1}(f(p_1))$.

To deal with invariance to rigid transformations and robustness to non-rigid ones, we compute the Reeb graph of the input 2-manifold (represented by a triangulation noted T) using a Morse function based on geodesic distances. In particular, to introduce some *visual semantic* in the decomposition, we automatically extract *feature points* [KLT05] (vertices located on the extremity of prominent components). For each vertex $v \in T$, $f(v) = \delta(v, v_f)$ where δ stands for the geodesic distance and v_f for the closest feature point from v. Figure 2(a) shows the level lines of f and the feature points of T (in green). For further details about the Reeb graph construction algorithm, we refer the reader to [TVD06].

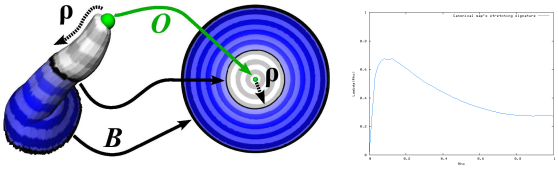

(a) (b)

Figure 3: *Disk-like chart unfolding signature computation.*

Definition 2 (Reeb chart) Let $\Psi : M \rightarrow R(f)$ map each point p of M to its equivalence class in $R(f)$. Let $E = \{E_0, \ldots E_n\}$ be the edges (maximally connected unions of equivalence classes containing only regular points) of the Reeb graph $R(f)$. $C_i = \Psi^{-1}(E_i)$ is defined as a *Reeb chart*.

Figure 2(b) shows a dual Reeb graph (where each edge E_i is collapsed in a colored node). Figures 2(c) and 2(d) show the segmentation of the hand model into its Reeb charts. Basically, Reeb charts are the partitions of the surface that correspond to the nodes of the dual Reeb graph.

Statement 1 (Reeb chart topology) Reeb charts of a compact closed orientable 2-manifold have either disk or annulus topology whatever the genus of the manifold is.

This statement can be briefly argued as follows. By definition, an edge E_i has two extremities, whose pre-images by Ψ are circles which form the boundaries of the chart C_i (C_i has genus zero). Hence, charts have two boundaries and thus annulus topology. However, for charts adjacent to a local extremum of f, the related boundary collapses to a point (the extremum). Thus that kind of chart is given disk topology.

In fig. 2(d), disk-like Reeb charts have been colored in blue and annulus-like ones in red. Notice that the proposed decomposition brings a certain *visual semantic*: each of the fingers of the hand model forms a distinct chart.

4. Reeb chart unfolding signatures

4.1. Disk-like Reeb chart unfolding

Given the segmentation provided by the Reeb graph, a straightforward and natural mapping to the canonical planar domain is used, without further computation cost, based on the Morse function represented by the Reeb graph. Indeed, for a disk-like Reeb chart C_i, let O be the local extremum of f it contains and B its boundary. We let ϕ_i map O to the center of the unit planar disk, B to its boundary and f level lines to concentric circles, as shown in fig. 3 where the thumb of the hand of fig. 2 has been mapped to the planar domain D.

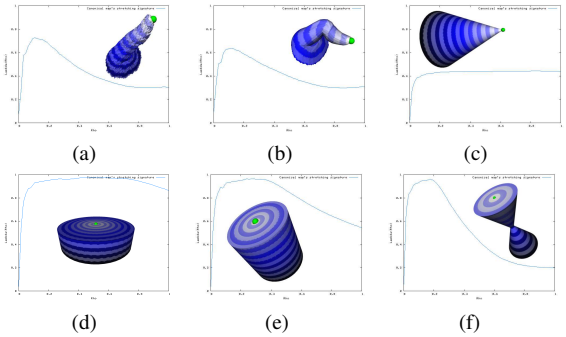

(a) (b) (c) (d) (e) (f)

Figure 4: *Example of stretching signatures for altered versions of the thumb chart and other primitive charts.*

Let $\rho(p) \in]0,1]$ be the normalized absolute difference of f values between O and a point $p \in C_i$, as shown in figure 3. Consequently to the Reeb chart definition, the sub-level sets of ρ have also disk topology, as illustrated by the white sub-level set in figure 3. In particular, as ρ increases, the shape of the sub-level sets varies. Thus it induces an evolution in the distortion introduced by their mapping to D. Consequently, to capture the evolution of the chart's shape variation, we propose to introduce the *stretching signature* λ_{ϕ_i} of ϕ_i as follows:

$$\lambda_{\phi_i}(\rho) = \frac{A_{C_i}(\rho)}{A_D(\rho)} = \frac{A_{C_i}(\rho)}{\pi\rho^2} \quad (1)$$

where $A_{C_i}(\rho)$ stands for the area of the sub-level set for parameter ρ on C_i and $A_D(\rho)$ stands for the area of the sub-level set on D. $A_{C_i}(\rho)$ is computed by summing the areas of the related triangles of T (after having normalized edge length by f, similarly to ρ). Roughly, $\lambda_{\phi_i}(\rho)$ depicts the *stretch* one has to apply on the chart to map it to a disk as ρ increases.

Figure 4 shows some examples of stretching signatures for various disk-like primitives. As f is based on geodesic distances, it is invariant to rigid transformations and robust to non-rigid transformations, as shown in figure 4(b), where the signature of a bent version of the thumb gives a signature nearly identical to the original. Moreover, it is also robust to surface noise, as shown in figure 4(a).

The close relationship between the stretching signature and the represented shape can be underlined by the following remarks. In figure 4(d), C_i is planar until $\rho = 0.65$, thus $\lambda_{\phi_i}(\rho)$ tends to 1 until $\rho = 0.65$. For a cone, $\lambda_{\phi_i}(\rho) = sin(\alpha)$ where $\alpha = atan(\frac{r}{h})$ where r and h stand for the radius and the height of the cone. Hence, $\lambda_{\phi_i}(\rho)$ tends to a constant term, as shown in figure 4(c). Finally, when a bottleneck is present on the chart (figure 4(f)), the signature describes an inflection.

4.2. Annulus-like Reeb chart unfolding

An analog reasoning can be applied for annulus-like charts. Let B_1 be the boundary of shortest perimeter of an annulus-like chart C_j and B_2 the other one. In this case, we let ϕ_j map B_1 to the inner boundary of the unit planar annulus and B_2 to its outer boundary, as shown in figure 5. By defining

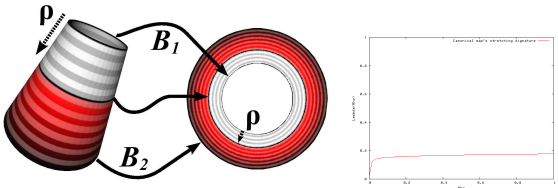

(a) (b)

Figure 5: *Annulus-like chart unfolding signature.*

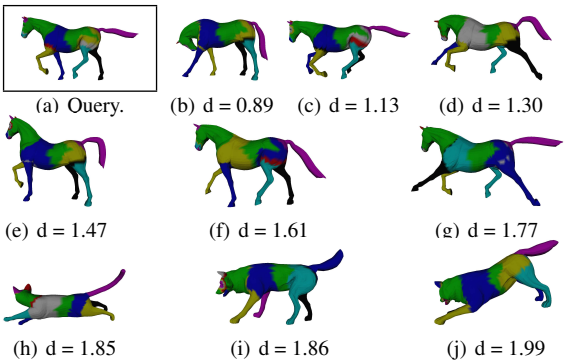

(a) Query. (b) d = 0.89 (c) d = 1.13 (d) d = 1.30
(e) d = 1.47 (f) d = 1.61 (g) d = 1.77
(h) d = 1.85 (i) d = 1.86 (j) d = 1.99

Figure 6: *Chart similarity matchings between a horse query model and retrieved results.*

the ρ parameter similarly to the previous paragraph, we can state that the sub-level sets of ρ have also annulus topology, as illustrated by the white sub-level set in figure 5. Hence, we introduce the stretching signature λ_{ϕ_j} of ϕ_j as follows, (1 is the inner radius of the unit annulus):

$$\lambda_{\phi_j}(\rho) = \frac{A_{C_j}(\rho)}{A_D(\rho)} = \frac{A_{C_j}(\rho)}{\pi(\rho+1)^2 - \pi} \quad (2)$$

Notice that in figure 5, the chart is based on a truncated version of a cone; thus its signature is similar to figure 4(c).

5. Application to pose-insensitive shape similarity

To assess the efficiency of the proposed signature, we use it for shape similarity estimation on the ISDB dataset from Tel-Aviv University, which is composed of articulated characters (106 surface models, 9 classes: cats, dinos, dogs, frogs, hands, horses, humans, lions and wolves).

5.1. Global shape similarity

First, for the comparison of two chart signatures, we use an L_1 distance, normalized by the number of samples in the signatures (typically 64). Then, to compute the distance between two models, we run a bipartite matching algorithm [TL07] that matches pairs of topology equivalent charts that minimize their distance, minimizing the overall sum of distances, noted d. Finally, the distance between two models is given by d. Thanks to the conciseness of the signatures, once the Reeb graph of the query has been computed, the shape comparison between the query and the whole dataset is achieved in about **100 milliseconds** (with a P4-CPU PC).

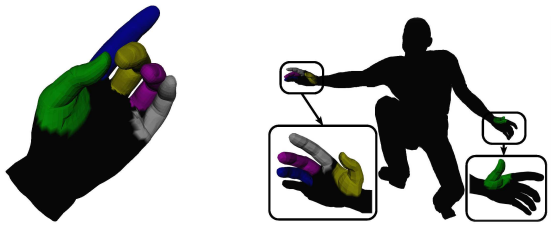

(a) (b)

Figure 7: *Chart similarity matchings between a hand and a human model.*

Figure 6 shows a typical query and the results retrieved by the system. Charts that have been matched together have been displayed with the same color. Notice that, except in one case, the tail of the horse query model has been matched with the tail of each retrieved result. Similar comments can be made for the legs, or the neck, which demonstrates the efficiency of the proposed signature. Moreover, this figure shows that the proposed signature is clearly pose-insensitive since horses in different poses have been retrieved as the top results. Table 1 gives a more quantitative evaluation of the system, with comparison to other techniques (the higher the scores are the better they are, see [SMKF04]). The first line reports the scores of our comparison algorithm, using Reeb chart unfolding signatures. The second one reports the scores of the same algorithm, using the sub-part attributes proposed in [HSKK01] (area ratio and Morse interval length). For example, with 1^{st} Tier score, the gain provided by Reeb chart unfolding signatures is about **9 %**. Notice that scores from [GSCO07] could not be reported as they were obtained on an unspecified subset of 80 models of the ISDB dataset.

Methods	NN	1^{st} T.	2^{nd} T.	E-M	DCG
RCU	**94.3 %**	**79.2 %**	**89.4 %**	**59.1 %**	**92.1 %**
HBA	88.7 %	70.6%	85.7 %	54.0 %	89.1 %
[FMK*03]	67.9 %	44.0 %	60.6 %	39.4 %	71.7 %

Table 1: *Similarity estimation scores on the ISDB dataset.*

5.2. Partial shape similarity

Figure 7 zooms in the chart matchings between a hand and a human surface model, displaying in color some of the charts that have been matched together. Notice that the thumb has been matched with the correct thumb of the humanoid and that the remaining fingers have been matched with fingers, despite their pose difference. In the future, based on this encouraging result, we would like to design a graph-based matching algorithm so that, for example, the hand model can be matched with its corresponding hand in the humanoid, achieving partial shape similarity [FKS*04].

6. Conclusion and future work

In this paper we proposed a novel surface parameterization based technique for pose-insensitive 3D shape signature, based on Reeb chart unfolding. It improves previous parameterization methods by being able to handle surfaces of arbitrary genus, using a divide-and-conquer strategy based on Reeb graphs. It also improves previous decomposition techniques, by providing a more efficient sub-part signature, resulting in better scores on the ISDB dataset (see table 1). However, when performing signature similarity evaluation, we did not take advantage of the intrinsic structural information brought by the Reeb graph, so as to underline the gain of the signatures only. In the future, we will focus on sub-graph matching algorithms to address the partial shape retrieval problem, benefiting from the efficient part matching proposed by Reeb chart unfolding signatures (fig. 7).

Acknowledgements

The authors would like to thank Ran Gal from Tel-Aviv University for providing the ISDB dataset. This work is partially supported by the European NoE *Delos* No. 507618.

References

[BMSF06] BIASOTTI S., MARINI S., SPAGNUOLO M., FALCIDIENO B.: Sub-part correspondence by structural descriptors of 3D shapes. *Computer-Aided Design Journal 38* (2006), 1002–1019.

[FKS*04] FUNKHOUSER T., KAZHDAN M., SHILANE P., MIN P., KIEFER W., TAL A., RUSINKIEWICZ S., DOBKIN D.: Modeling by example. *ACM Transactions on Graphics 23* (2004), 652–663.

[FMK*03] FUNKHOUSER T., MIN P., KAZHDAN M., CHEN J., HALDERMAN A., DOBKIN D.: A search engine for 3D models. *ACM Transactions on Graphics 22* (2003), 83–105.

[GSCO07] GAL R., SHAMIR A., COHEN-OR D.: Pose oblivious shape signature. *IEEE Transactions on Visualization and Computer Graphics 13* (2007), 261–271.

[HSKK01] HILAGA M., SHINAGAWA Y., KOHMURA T., KUNII T.: Topology matching for fully automatic similarity estimation of 3D shapes. In *SIGGRAPH* (2001), pp. 203–212.

[KLT05] KATZ S., LEIFMAN G., TAL A.: Mesh segmentation using feature point and core extraction. *The Visual Computer 21* (2005), 865–875.

[PSF04] PATANÈ G., SPAGNUOLO M., FALCIDIENO B.: Paragraph: Graph-based parameterization of triangle meshes with arbitrary genus. *Computer Graphics Forum 23* (2004), 783–797.

[SMKF04] SHILANE P., MIN P., KAZHDAN M., FUNKHOUSER T.: The Princeton shape benchmark. In *IEEE Shape Modeling International* (2004), pp. 167–178.

[TL07] TAM G. K. L., LAU R. W. H.: Deformable model retrieval based on topological and geometric signatures. *IEEE Transactions on Visualization and Computer Graphics 13* (2007), 470–482.

[TVD06] TIERNY J., VANDEBORRE J.-P., DAOUDI M.: 3D mesh skeleton extraction using topological and geometrical analyses. In *Pacific Graphics* (2006), pp. 85–94.

[WWJ*06] WANG S., WANG Y., JIN M., GU X., SAMARAS D.: 3D surface matching and recognition using conformal geometry. In *IEEE CVPR* (2006), pp. 2453–2460.

[ZMT05] ZHANG E., MISCHAIKOW K., TURK G.: Feature-based surface parametrization and texture mapping. *ACM Transactions on Graphics 24* (2005), 1–27.